Development 133, 4749-4759 (2006) doi:10.1242/dev.02665

Frizzled3a and Celsr2 function in the neuroepithelium to regulate migration of facial motor neurons in the developing zebrafish hindbrain

Hironori Wada[1], Hideomi Tanaka[1,2], Satomi Nakayama[1], Miki Iwasaki[1,2] and Hitoshi Okamoto[1,2,*]

Migration of neurons from their birthplace to their final target area is a crucial step in brain development. Here, we show that expression of the *off-limits/frizzled3a* (*olt/fz3a*) and *off-road/celsr2* (*ord/celsr2*) genes in neuroepithelial cells maintains the facial (nVII) motor neurons near the pial surface during their caudal migration in the zebrafish hindbrain. In the absence of *olt/fz3a* expression in the neuroepithelium, nVII motor neurons extended aberrant radial processes towards the ventricular surface and mismigrated radially to the dorsomedial part of the hindbrain. Our findings reveal a novel role for these genes, distinctive from their already known functions, in the regulation of the planar cell polarity (i.e. preventing integration of differentiated neurons into the neuroepithelial layer). This contrasts markedly with their reported role in reintegration of neuroepithelial daughter cells into the neuroepithelial layer after cell division.

KEY WORDS: Zebrafish, *frizzled*, *celsr*, Facial motor neuron, Neuroepithelium

INTRODUCTION

Migration of immature neurons from their site of origin to their final destination is a crucial step in the development of the vertebrate nervous system. Many neurons migrate tangentially through one cell layer at a specific depth within the brain. Some neurons migrate through the subventricular region (e.g. the GABAergic neurons into the olfactory bulb); others migrate near the pial surface (e.g. the granule cells into the cerebellar cortex), or through the intermediate zone (e.g. the GABAergic neurons into the cerebral cortex) (reviewed by Kriegstein and Noctor, 2004; Hatten, 2002). The mechanisms by which neurons select specific layers as their migrating pathway remain largely unknown.

The zebrafish is a good model to address this issue. In the developing zebrafish hindbrain, the facial (nVII) motor neurons originate in rhombomere (r)4 and migrate caudally to r6, where they form the facial motor nucleus (Chandrasekhar et al., 1997; Higashijima et al., 2000). These neurons migrate near the pial surface of the hindbrain (Wada et al., 2005). Several molecules that regulate the migration of nVII motor neurons have been identified in our, and other, laboratories. The *trilobite/strabismus* (*tri/stbm*; *stbm* is also known as *vangl2* – Zebrafish Information Network) and *prickle1* (*pk1*) genes, originally identified in *Drosophila* as planar cell polarity (PCP) genes (reviewed by Tree et al., 2002; Klein and Mlodzik, 2005), regulate caudal migration of the nVII motor neurons (Bingham et al., 2002; Jessen et al., 2002; Carreira-Barbosa et al., 2003). We have previously shown that a cytoplasmic protein Landlocked/Scribble1 (Llk/Scrb1) is required for migration of the nVII motor neurons and that it genetically interacts with Tri/Stbm during convergent extension (CE) movements (Wada et al., 2005). A recent study has shown that the *tri/stbm* gene controls the anterior-posterior polarity of the neuroepithelial cells to regulate their reintegration in the zebrafish spinal cord after cell division (Ciruna et al., 2006). Thus, the neuroepithelial cells may regulate migration of nVII motor neurons through their polarized activity mediated by these gene products. However, the mechanisms by which these molecules regulate neuronal migration have not been investigated.

Here, we demonstrate that expression of the *off-limits/frizzled3a* (*olt/fz3a*) and *off-road/celsr2* (*ord/celsr2*) genes in neuroepithelium maintains the nVII motor neurons near the pial surface during their caudal migration in the zebrafish hindbrain. In the absence of *olt/fz3a* expression in the neuroepithelium, the nVII motor neurons failed to migrate caudally; instead, they migrated radially into the dorsomedial part of the hindbrain by extending aberrant radial processes. Mosaic analyses showed that expression of the *olt/fz3a* gene in the surrounding neuroepithelial cells prevented integration of the nVII motor neurons into the neuroepithelial layer.

MATERIALS AND METHODS

Zebrafish strains and mutagenesis

Zebrafish (*Danio rerio*) were maintained according to standard protocols (Westerfield, 2000). The zebrafish Isl1-GFP transgenic line (registered as *Tg(CM-isl1:GFP)^{rw0}* in the Zebrafish National BioResource Project of Japan, http://www.shigen.nig.ac.jp/zebra/index_en.html) (Higashijima et al., 2000) was derived from the RIKEN-Wako wild-type strain. The WIK strain was used for genetic mapping (Shimoda et al., 1999). Mutagenesis using *N*-ethyl-*N*-nitrosourea (ENU) has been described previously (Wada et al., 2005). One allele for the *olt* locus (*olt^{rw689}*) and four alleles for the *ord* locus (*ord^{rw71}*, *ord^{rw135}*, *ord^{rw166}* and *ord^{rw380}*) were identified and used in this study. All embryos used in this study carried the Isl1-GFP transgene. Images were captured using a fluorescent dissecting microscope (Leica MZFLIII) with a CCD camera (Hamamatsu C5810). All strains are available from the Zebrafish National BioResource Project of Japan.

Mapping of the mutant loci

Genetic mapping of the mutant loci was carried out as described previously (Wada et al., 2005). In total, 463 *olt* and 1027 *ord* homozygous embryos were used to assign the locus to a linkage group. Expressed sequence tags (ESTs) and genomic sequences were obtained from the T51 radiation hybrid panel (Research Genetics, http://www.resgen.com/) and the Sanger Centre genome database (http://www.ensembl.org/index.html). The SSLP markers mrck1 and wz12343 were generated based on the sequences of a putative gene annotated as *myotonin-related Cdc42-binding kinase* (*mrck*)α and an EST (wz12343), respectively (Table 1).

[1]Laboratory for Developmental Gene Regulation, Brain Science Institute, The Institute of Physical and Chemical Research (RIKEN), 2-1 Hirosawa, Wako, Saitama 351-0198, Japan. [2]Core Research for Evolutional Science and Technology (CREST), Japan Science and Technology Corporation (JST), 4-1-8 Honcho, Kawaguchi, Saitama, 332-0012, Japan.

*Author for correspondence (e-mail: hitoshi@brain.riken.jp)

Accepted 28 September 2006

Table 1. Nucleotide sequences of the primers and antisense morpholino origonucleotides MOs used in this study

Primers	
Primers used for the amplification of the SSLP markers	
mrck1	5′-TTAATGATGTGCTGACGCAGG-3′
	5′-GCACAAGTACAGTGTTGGTCG-3′
wz12343	5′-CATCAGCGTACACACGAACT-3′
	5′-CAGATATCGCCAACAGTGCA-3′
Primers used for the amplification of the partial cDNA to generate RNA probes	
fz3a	5′-GTGTGGAGGAGCGCGTTTCTC-3′ (sense)
	5′-TGAGGCTGTGGGTTCAATTCC-3′ (antisense)
celsr1a	5′-GTTGGTTATTATGGGTTCACC-3′ (sense)
	5′-TCCAAACAGTACGCGTCCTTC-3′ (antisense)
celsr1b	5′-CAGTGATATGGATGTGCTTCG-3′ (sense)
	5′-CTCATCTCGCTGATTGTGAGG-3′ (antisense)
celsr2	5′-GGGTCCCCAAACTGCCTGAGG-3′ (sense)
	5′-CACCAGCCACGCGGACACGGC-3′ (antisense)
celsr3	5′-CAAAATGGCGGCACATGTCGG-3′ (sense)
	5′-CTGTGGGTGGGGCAAGGGGAG-3′ (antisense)
Primers for RT-PCR assay to show splicing defects induced by the MOs	
fz3a	5′-ATGCTGACTGTATGCATGGCC-3′
	5′-GCCATAATCCCGTTGAACTGC-3′
celsr1a	5′-GATGACAACATCTGCCTAAGG-3′
	5′-GACTAGCAGGTTGACACACTC-3′
celsr1b	5′-CATTTGTGGCGTCTAATACAG-3′
	5′-GGCTTCTCGTACTCTCCGTCG-3′
celsr2	5′-TTCGTGACGTCCGACACCATC-3′
	5′-GAAGGTGATGAAGGTCTGCGG-3′
MOs	
fz3a-MO	5′-CAATGTGAATTGGTTTACCTCCATG-3′
celsr1a-MO	5′-CATTTAGCAAACTCACCTGTGAAGT-3′
celsr1b-MO	5′-TAAGAGAATGACTGACCTGTAAAAT-3′
celsr2-MO	5′-GAGGCTCCGCCCTCACCTGTGTAGT-3′
Control MOs	
fz3a-MO-5mis	5′-CAAaGTcAATTGcTTTACgTCgATG-3′
celsr1a-MO-5mis	5′-CATTTAcCAAAgTCACaTGTcAAcT-3
celsr1b-MO-5mis	5′-TAAGAcAATcACTcACCTcTAAtAT-3′
celsr2-MO-5mis	5′-GAGcCTgCGCCCTCAgCTcTGTAcT-3′

Underlined text indicates exons. Lower-case letter indicate mispaired residues.

Identification of the genes

To isolate the *fz3a*, *fz3b* and *celsr2* genes, total RNA was extracted from 24-hours post-fertilization (hpf) homozygous mutant embryos using an RNA extraction kit (Nippon gene). cDNAs were amplified by PCR using a first-strand cDNA synthesis kit (Takara) and specific primers designed according to genomic sequences from the Sanger Centre genome database. The amino acid sequences were deduced from the nucleotide sequences of partial cDNAs. To confirm the nucleotide changes in the mutant alleles, genomic DNA from grandparents of the family containing the mutations were also sequenced. The phylogenetic relationship among family genes was analyzed using the CLUSTAL W program at the DDBJ (http://www.ddbj.nig.ac.jp/search/clustalw-e.html). The following amino acid sequences were used for comparison: mouse (m) Fz8 (accession number, Q61091); mFz3 (Q61086); human (h) Fz3 (AAF89088); *Xenopus* (x) Fz3 (ZAA04977); mCelsr1 (NP_536685); mCelsr2 (NP_059088); and mCelsr3 (NP_034016). In the analyses, total lengths were used for the Frizzled family proteins and the extracellular regions were used for the Celsr family proteins. For in situ hybridization, we used partial cDNA fragments PCR-amplified from the *fz3a* gene (517 bp corresponding to the 3′-terminal region), the *celsr2* gene (1057 bp encompassing exons 8-11), the *celsr1a* gene (565 bp corresponding to the N-terminal region), the *celsr1b* gene (560 bp corresponding to the N-terminal region) and the *clsr3* gene (674 bp encompassing exons 8-11) (see Table 1). The PCR products were cloned into the TA cloning vector, pCRII-TOPO (Invitrogen), and sequenced using a BigDye terminator cycle sequencing kit (PE Applied Biosystems) with a DNA sequencer (ABI PRISM/3100 Genetic Analyzer). The accession numbers of *celsr2*, *celsr3*, *fz3a* and *fz3b* are AB246774, AB246775, AB246776 and AB246777, respectively.

Immunohistochemistry, in situ hybridization and retrograde cell labeling

Immunohistochemistry was performed according to standard protocols (Westerfield, 2000), using anti-acetylated α-tubulin antibody (Sigma, diluted 1:1000), zn-5-antibody (Oregon Monoclonal Bank, diluted 1:100) (Trevarrow et al., 1990), anti-β-catenin antibody (Sigma, diluted 1:500) and a secondary antibody conjugated to Alexa-533 (Santa Cruz Biotechnology, diluted 1:500). The samples were viewed under confocal microscopy (Zeiss LSM 510). Isl1-GFP signals were captured simultaneously in the samples. In situ hybridization using RNA probes was carried out as described (Westerfield, 2000). To monitor hindbrain differentiation, we used RNA probes for *tag1* (also known as *cntn2* – Zebrafish Information Network) (Warren, Jr et al., 1999), *hoxb1a* (Prince et al., 1998), *krox20* (Oxtoby and Jowett, 1993) and *val/mafb* (Moens et al., 1998). Images were captured using a differential interference contrast microscope (Zeiss Axioplan2) with a CCD camera (Olympus DP50). Retrograde labeling of the reticulospinal neurons and the octavolateralis (OLe) neurons was carried out as described previously (Wada et al., 2005). At least ten embryos were monitored in each experiment.

Gene knockdown

Antisense morpholino oligonucleotides (MO) to target the first exon/intron boundary of *fz3a*, and the second exon/intron boundary of *celsr2*, *celsr1a* and *celsr1b* were designed by Gene Tools (see Table 1 and Fig. S2D,I in the supplementary material). Approximately 1 nl of MO (5 mg/ml) was injected into one-cell-stage embryos (5 ng per embryo), as described (Nasevicius and Ekker, 2000). RT-PCR assay was carried out to confirm the splicing defects of the MOs, as described (see Fig. S2E,J in the supplementary material) (Goutel et al., 2000).

Injection of mRNA and detection of the expressed proteins

The wild-type *fz3a*, the mutated *fz3a*^{rw689} and the truncated *fz3a*-ΔC (1515 bp, which lacks the cytoplasmic region) cDNAs were amplified by RT-PCR and subcloned into pCS2 expression vectors. Sense-capped mRNA was synthesized using a mMessage mMachine kit (Ambion). Approximately 1 nl of mRNA (0.5 mg/ml) was injected into one-cell-stage embryos (0.5 ng per embryo). To monitor the subcellular localization of the expressed proteins, Venus-fused cDNAs (*fz3a-venus* and *fz3a*^{rw689}*-venus*) were generated (Nagai et al., 2002) and the corresponding mRNA was injected into one-cell-stage embryos, as described. To monitor the subcellular localization of Deshevelled (Dsh), mRNA encoding Xdsh:GFP (Rothbacher et al., 2000) was co-injected with *fz3a* or *fz3a*^{rw689} mRNAs. For each construct, five embryos were monitored under confocal microscopy at 10-12 hpf.

Cell transplantation

Cell transplantation was performed as described (Wada et al., 2005; Moens et al., 1996). MZ-*olt*^{rw689} and MZ-*ord*^{rw71} embryos were produced by homozygous crosses. Live mosaic embryos were analyzed at 36-48 hpf. To confirm that the transplanted donor cells developed into nVII motor neurons, we monitored peripheral axons from donor cells labeled with rhodamine, as described previously (Wada et al., 2005). We used IMARIS 4.2 software (Bitplane) to visualize mosaicism and optical sections in the neuroepithelium.

Time-lapse observations

The procedures for time-lapse observations were essentially the same as described (Langenberg et al., 2003; Bingham et al., 2005) with modifications (H.T. and H.O., unpublished). Briefly, the hindbrain regions were excised with a fine blade from embryos at 18 hpf. The resulting hindbrain explants were embedded in 1.5% agarose in a small chamber and covered with L-15 medium (Gibco BRL) supplemented with penicillin/streptomycin cocktail (Gibco BRL). The chamber was sealed with a cover slip and observed under

confocal microscopy every 10 minutes at 18-33 hpf (lateral views) or 18-22 hpf (cross sections). Five samples were analyzed in each experiment. Aberrant radial processes of the nVII motor neurons were counted in live embryos at 20-22 hpf.

RESULTS

The genes affected in the *olt* and *ord* mutants are specifically required for caudal migration of the nVII motor neurons

We previously used the zebrafish Isl1-GFP transgenic line, which expresses green fluorescent protein (GFP) in the branchiomotor neurons of the hindbrain (Higashijima et al., 2000), to identify novel mutants with perturbed caudal migration of the nVII motor neurons (Wada et al., 2005). The *olt* and *ord* mutations were further characterized, and one allele for the *olt* locus (*olt*^{rw689}) and four alleles for the *ord* locus (*ord*^{rw71}, *ord*^{rw135}, *ord*^{rw166} and *ord*^{rw380}) were used in this study.

In wild-type embryos, the nVII motor neurons begin to express GFP in r4 at 16 hours post-fertilization (hpf), after which they start migrating caudally towards r6 (Fig. 1D,G) (Chandrasekhar et al., 1997; Higashijima et al., 2000; Wada et al., 2005). The *olt* and *ord* embryos display impairment in migration of the nVII motor neurons, albeit differently. In the *olt* embryos, none of the nVII motor neurons migrated caudally, but they all migrated dorsally into r4 (Fig. 1E,H). By contrast, in the *ord* embryos, some of the nVII motor neurons also migrated into the r5 region (Fig. 1F,I). Embryos homozygous for each of the four alleles of *ord* showed similar impairment in migration of the nVII motor neurons. The other morphological features of the *olt* and *ord* embryos were normal as compared to those of wild-type embryos (Fig. 1A-C), and the adult mutants were viable and fertile. We obtained maternal-and-zygotic (MZ) embryos by mating homozygous fish. Because the MZ-*olt*^{rw689} and MZ-*ord*^{rw71} embryos were also viable and displayed the same defects in neuronal migration, we used them in the subsequent analyses. In the following experiments, we showed that the *ord* and *olt* genes are barely expressed maternally (see below and Fig. S2C,G in the supplementary material). These results suggest that these genes are not required in the early stages of development, supporting the viability of the MZ-*olt*^{rw689} and MZ-*ord*^{rw71} embryos.

Despite their ectopic localization, nVII motor neurons in the mutant embryos expressed *tag-1* mRNA and extended peripheral axons normally to the correct target muscles (see Fig. S1A-F in the supplementary material). Moreover, the expression patterns of the rhombomere-specific genes and the formation of hindbrain neurons appeared unaffected in the mutant embryos (see Fig. S1G-U in the supplementary material). These results suggest that the overall patterning and differentiation of the hindbrain neurons were unaffected by the mutation, except for the aberrant migration of the nVII motor neurons.

olt encodes zebrafish Frizzled3a

The *olt* locus was genetically mapped to the linkage group 20 (Fig. 2A). This genomic region contains a gene similar to mammalian *frizzled3* (Fig. 2B,C) (Wang et al., 2002). Because another *frizzled3* homolog was identified (Fig. 2D), we termed the gene associated with the *olt* locus zebrafish *frizzled3a* (*fz3a*) and the other homolog *frizzled3b* (*fz3b*). Sequence analyses showed that the allele *olt*^{rw689} carries a mis-sense mutation resulting in substitution of the second conserved cysteine of the extracellular cysteine-rich domain (CRD) of Fz3a (C38S) (Fig. 2C; see also Fig. S2A in the supplementary material). This amino acid substitution may disrupt proper folding, and thereby the function, of the Frizzled family proteins, because the

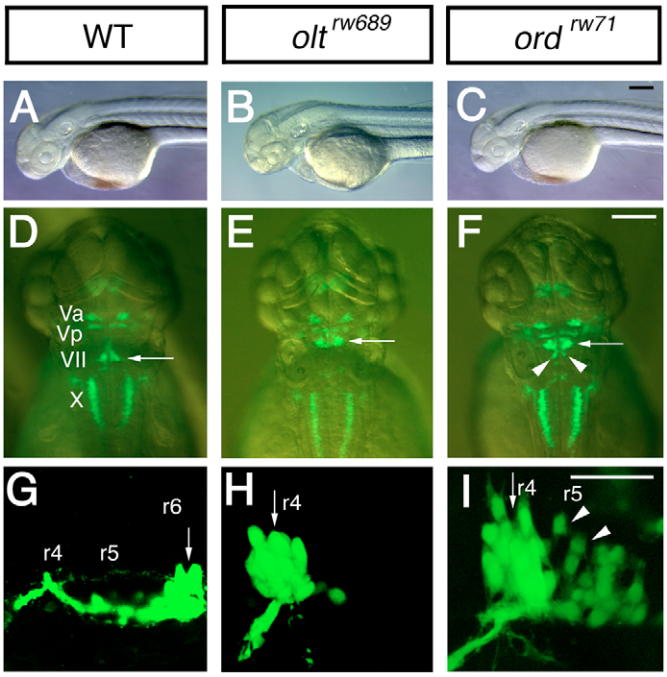

Fig. 1. *olt* and *ord* genes are required for migration of nVII motor neurons. (**A-I**) Morphology and Isl1-GFP expression of wild-type (A,D,G), MZ-*olt*^{rw689} (B,E,H) and MZ-*ord*^{rw71} (C,F,I) Isl1-GFP embryos at 48 hpf (A-F) and 30 hpf (G-I). In wild-type embryos (D,G), the nVII motor neurons are located in r6 (arrows). By contrast, in *olt* (E,H) and *ord* (F,I) embryos, most or all of the neurons are located in r4 (arrows). In *ord* embryos (F,I), some neurons migrate into r5 (arrowheads). (A-C,G-I) Lateral views; anterior facing left. (D-F) Dorsal views; anterior at the top. (A-F) Images obtained using a dissecting microscope. (G-I) Composite images of serial optical sections obtained by confocal microscopy. Va, anterior trigeminal nuclei; Vp, posterior trigeminal nuclei; VII, facial nucleus; X, vagus nucleus. Scale bars: 50 μm. The images in A,C,D,F,G,I were previously published in Wada et al. (Wada et al., 2005).

second and fourth conserved cysteines of the CRD form a disulfide bond (Dann et al., 2001). Indeed, in *Drosophila*, the mutated Dfz2^{C3}, which carries a substitution of the fourth conserved cysteine of the CRD to serine (C118S), shows a reduced capacity to reach the cell surface (Chen et al., 2004). Ectopically expressed Frizzled family proteins recruit the downstream effector Dsh to the plasma membrane (Axelrod et al., 1998), and recruitment of Dsh to the plasma membrane is essential for downstream signaling (Park et al., 2005). Thus, to determine whether the amino acid substitution resulting from the mutation in the *ord*^{rw689} allele leads to functional disruption of the Fz3a protein, we examined the subcellular localization of Fz3a and mutated Fz3a^{rw689}, and of *Xenopus* Dsh (Xdsh), when Fz3a or Fz3a^{rw689} is overexpressed. We found that the mutated Fz3a^{rw689} protein was not associated with the plasma membrane and that it lost its capacity to recruit Xdsh to the plasma membrane (see Fig. S2B in the supplementary material).

To confirm that the loss of function of the *fz3a* gene is responsible for the *olt* phenotype, we used an antisense MO (*fz3a*-MO) (see Fig. S2D,E in the supplementary material). The resulting morphant phenotype was identical to that of the *olt* mutant embryos (Fig. 2F-H), with impaired migration of the nVII motor neurons (100% of MO-injected embryos; *n*=47). Control MO (*fz3a*-MO-5mis) did not impair migration of the nVII motor neurons in the injected embryos (*n*=30). There was little expression of *fz3a* mRNA up to the gastrula

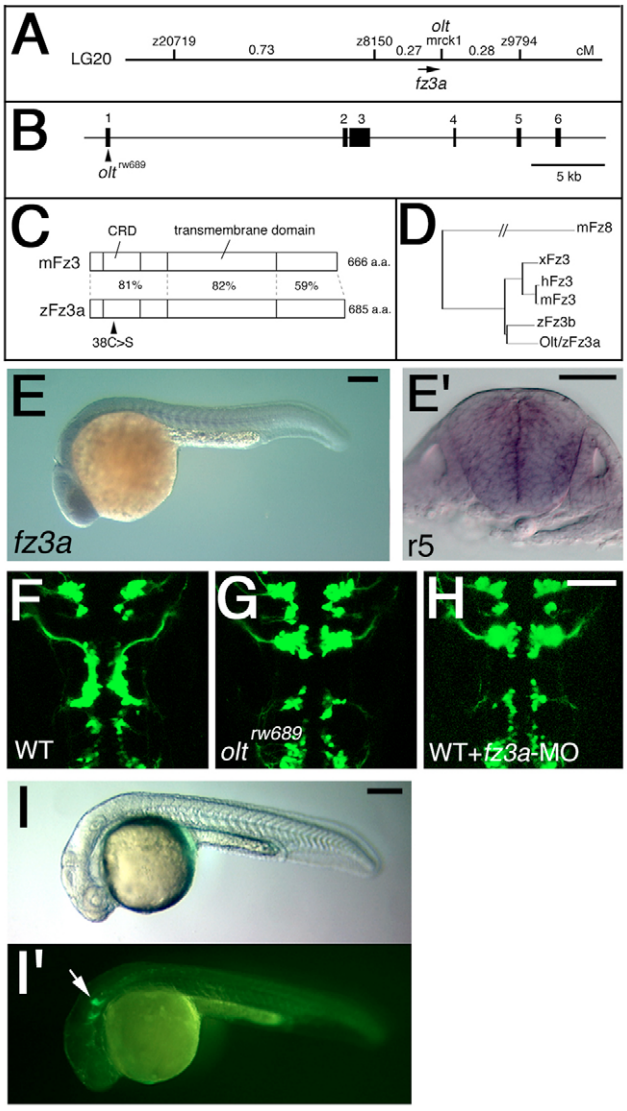

Fig. 2. Identification of the *olt* gene as zebrafish *frizzled3a* gene. (**A**) Genetic map of the *olt* locus. (**B**) Genomic structure of the zebrafish *fz3a* gene. The nucleotide substitution resulting from the *olt*^{rw689} mutation is indicated. (**C**) Schematic drawings for the mouse Fz3 and zebrafish Fz3a proteins. Amino acid sequence similarity (%) is shown for each domain. The mis-sense amino acid substitution in the Fz3a^{rw689} protein is indicated. (**D**) The phylogenetic tree for fz3-family genes. (**E**) Lateral view of a wild-type embryo reacted with the *fz3a* RNA probe at 24 hpf. (**E′**) Cross section of E at r5. (**F-H**) Wild-type Isl1-GFP embryo injected with *fz3a*-MO (H) showing the same neuronal migration defects as those observed in an *olt* embryo (G). The embryos are shown in dorsal view and the images are composite stacks of serial optical sections. (**I,I′**) Wild-type Isl1-GFP embryo injected with *fz3a*-ΔC mRNA. Migration of the nVII motor neurons was specifically impaired (arrow in I′). Lateral views. Scale bars: 50 μm.

stages (see Fig. S2C in the supplementary material), but *fz3a* mRNA was expressed throughout the hindbrain at 24 hpf, at the time when the nVII motor neurons are migrating (Fig. 2E,E′).

Next, we analyzed whether injection of *fz3a* mRNA could rescue the neuronal migration defects in the *olt* embryos. However, injection of *fz3a* mRNA into the wild-type or *olt* embryos caused general malformation, including the severe disruption of brain structures (data not shown; 100% of injected embryos; 62 wild-type and 46 *olt* embryos). By contrast, when we injected a truncated form of *fz3a* mRNA (*fz3a*-ΔC) lacking the C-terminal intracellular domain, a significant proportion of embryos showed loss of nVII motor-neuron migration, without early pattern formations or CE movements being affected (Fig. 2I,I′; 36% of injected embryos, *n*=55). These results demonstrated that Fz3a-ΔC acts dominant-negatively in a highly specific manner, confirming the specific role of the *fz3a* gene in the migration of nVII motor neurons.

ord encodes zebrafish Celsr2

The *ord* locus was genetically mapped to linkage group 22 (Fig. 3A). We showed that this genomic region contains a gene coding for Celsr2 (for cadherin, EGF-like, LAG-like and seven-pass receptor), which is a vertebrate homolog of *Drosophila* Flamingo (Fmi, also known as Stan – Flybase) (Fig. 3B-D) (Usui et al., 1999; Formstone and Little, 2001; Shima et al., 2002). Sequence analyses showed that each of the four alleles of the *ord* locus carries a point mutation in the *celsr2* gene. The alleles *ord*^{rw71}, *ord*^{rw166} and *ord*^{rw380} carry a mis-sense mutation resulting in amino acid substitution (C1835S, E582K and V1168D, respectively) in the extracellular domain, and the *ord*^{rw135} allele carries a premature stop codon (L288Stop) in the extracellular domain (Fig. 3C, see also Fig. S2F in the supplementary material).

To confirm that loss of function of the *celsr2* gene is responsible for the *ord* phenotype, we used an antisense MO (*celsr2*-MO) (see Fig. S2I,J in the supplementary material). The resulting morphant phenotype was identical to that of the *ord* mutant embryos (Fig. 3H-J), with impaired migration of the nVII motor neurons (95% of MO-injected embryos; *n*=99), confirming that the *ord* gene encodes Celsr2. Migration of the nVII motor neurons was not impaired in 74 embryos injected with control MO (*celsr2*-MO-5mis). The *celsr2* mRNA was expressed throughout the embryo at the gastrula stages, and became restricted to the CNS thereafter (see Fig. S2G in the supplementary material). The *celsr2* mRNA was expressed throughout the brain at 24 hpf, when the nVII motor neurons were migrating (Fig. 3E,E′).

celsr1a and *celsr1b* function redundantly with *ord*/*celsr2* in regulating migration of the nVII motor neurons

The *celsr1*, *celsr2* and *celsr3* mRNAs are differentially expressed in developing mouse CNS (Formstone and Little, 2001; Shima et al., 2002). To understand the function of zebrafish celsr homologs in migration of the nVII motor neurons, we identified celsr family genes. A BLAST homology search and phylogenetic tree analyses revealed that two *celsr1* orthologs and one *celsr3* ortholog exists in the zebrafish genome (Fig. 3D). The *celsr1* orthologs have been described and referred to previously as *flamingo* (*fmi*)*1a* and *fmi1b* (Formstone and Mason, 2005). To abide by the rule of the Zebrafish Nomenclature Committee (http://zfin.org/zf_info/nomen.html) to follow the mammalian terminology, we refer to these genes as *celsr1a* (equivalent to *fmi1a*) and *celsr1b* (equivalent to *fmi1b*) in this study. We demonstrated that *celsr1a* and *celsr1b* mRNAs, but not *celsr3* mRNA, were also expressed in the developing hindbrain (Fig. 3F,F′,G,G′ and Fig. S2H in the supplementary material). We therefore analyzed the function of the *celsr1a* and *celsr1b* genes.

We designed *celsr1a*-MO and *celsr1b*-MO (see Fig. S2I,J in the supplementary material). Injection of *celsr1a*-MO or *celsr1b*-MO alone into wild-type embryos did not cause any defect in neuronal migration (Fig. 3L). However, co-injection of *celsr1a*-MO and *celsr1b*-MO gave rise to a phenotype similar to that of the *ord* embryos, showing impaired migration of the nVII motor neurons (34% of injected embryos, *n*=82; Fig. 3L). Interestingly, injection of

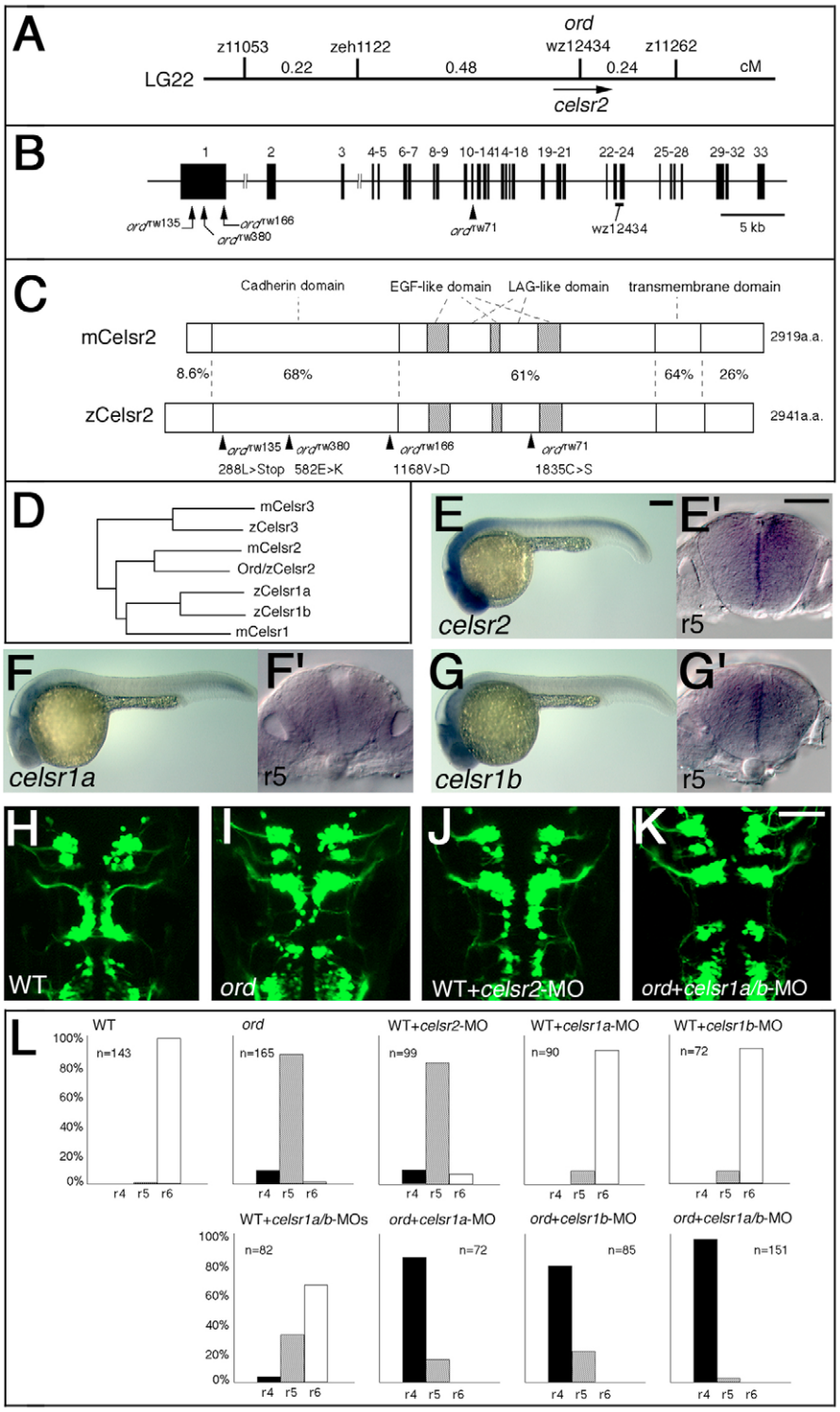

Fig. 3. Identification of the *ord* gene as zebrafish *celsr2* gene. (**A**) Genetic map of the *ord* locus. (**B**) Genomic structure of the zebrafish *celsr2* gene. The nucleotide substitution resulting from each mutation is indicated. (**C**) Schematic drawings of the mouse and zebrafish Celsr2 proteins. Amino acid sequence similarity (%) is shown for each domain. The amino acid substitution resulting from each mutation is indicated. (**D**) The phylogenetic tree for celsr-family genes. (**E-G**) Lateral views of wild-type embryos reacted with RNA probes for *celsr2* (E), *celsr1a* (F) and *celsr1b* (G) at 24 hpf. (**E′**,**F′**,**G′**) Cross sections at r5 for each embryo, E-G, respectively. (**H-K**) A wild-type Isl1-GFP embryo injected with *celsr2*-MO (J) shows incomplete disruption of the neuronal migration as observed in an *ord* embryo (I). (K) An *ord* mutant embryo injected with *celsr1a/1b*-MOs shows complete loss of migration of the nVII motor neurons. The embryos are shown in dorsal view and the images are composite stacks of serial optical sections. (**L**) The neuronal migration phenotype in each experiment was scored as follows: r4, complete loss of migration, as shown in K; r5, partial disruption of migration, as shown in I; and r6, normal migration, as shown in H. Scale bars: 50 μm.

celsr1a-MO or *celsr1b*-MO into the MZ-*ord* embryos enhanced the severity of neuronal migration defects. In most of the resulting embryos, the nVII motor neurons did not migrate at all (79% of embryos injected with *celsr1a*-MO, *n*=85; 85% of embryos injected with *celsr1b*-MO, *n*=72; Fig. 3L). Moreover, co-injection of *celsr1a*-MO and *celsr1b*-MO resulted in complete loss of neuronal migration in all the MZ-*ord* embryos, as observed in the *olt* embryos (97%, *n*=151; Fig. 3K,L,). Control MOs did not enhance the severity of neuronal migration defects in the MZ-*ord* embryos (none of the 71 embryos injected with *celsr1a*-MO-5mis, or of the 60 embryos injected with *celsr1b*-MO-5mis). These results suggest that *celsr1a* and *celsr1b* act in concert with *ord/celsr2* to regulate migration of the nVII motor neurons.

In mutant embryos, nVII motor neurons migrate aberrantly away from the pial surface of the hindbrain

To understand the function of the *fz3a* and *celsr2* genes, we characterized the migration of the nVII motor neurons in further detail. Wild-type and mutant embryos were stained with anti-

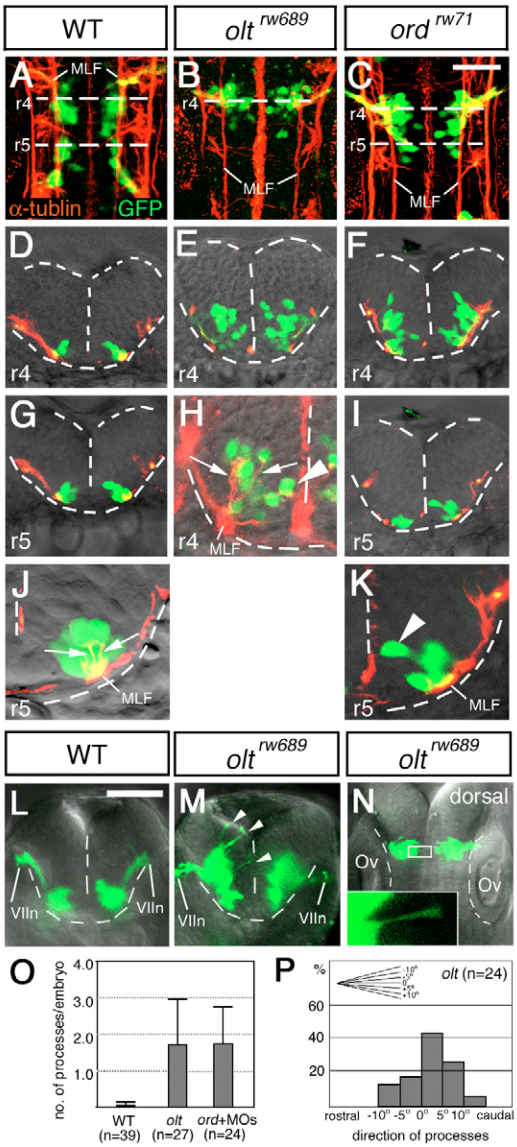

Fig. 4. Defective migration of the nVII motor neurons in mutant embryos. (**A-K**) Wild-type (A,D,G,J), *olt*^{rw689} (B,E,H) and *ord*^{rw71} (C,F,I,K) Isl1-GFP embryos were stained with anti-acetylated α-tubulin antibody. (A-C) Composite stacks of serial optical sections, shown in dorsal view. (D-K) Images are single focal planes of cross sections at the rhombomeric regions indicated by broken lines in A-C. Hindbrain regions are outlined by broken lines. (H,J,K) Higher magnifications of E, G, I, respectively. In the mutant embryos, some of the neurons reach the ventricular surface (arrowheads in H and K). However, these mismigrated neurons extend axons normally (shown by arrows in H and J). GFP-expression in single axons was barely detectable (H). Therefore, the yellow signals of the axons of the nVII motor neurons in the wild-type embryos (J) are technical artifacts caused by superimposition of the red signals of the axons and the green signals of the cell bodies of the overlapping neurons. (**L-P**) Aberrant radial processes in the mutant embryos (arrowheads in M). Frontal views of the live wild-type (L) and *olt* (M) Isl1-GFP embryos at r4, and a dorsal view of the *olt* Isl1-GFP embryo (N) at 24 hpf. Higher magnification of the boxed region is shown in the inset. (L-N) Images are composite stacks of serial optical sections. (O) Scoring of aberrant processes in the wild-type (WT), *olt* and *ord* embryos injected with *celsr1a/1b*-MOs (*ord*+MOs). Bars represent S.D. (P) Direction of the aberrant processes was quantified in the *olt* embryos. The angle of each process was measured as the deviation from the right angle to the midline. Scale bars: 50 μm.

acetylated α-tubulin antibody (red), and the Isl1-GFP signals (green) were captured simultaneously (Fig. 4A-K). The peripheral axons of the nVII motor neurons and the medial longitudinal fascicles (MLF) were immunoreactive to anti-acetylated α-tubulin antibody (Fig. 4A-K). In the wild-type embryos, the migrating motor neurons were localized close to the pial surface of the hindbrain and were connected to the MLF (Fig. 4A,D,G). Some of the migrating nVII motor neurons appeared to be in direct contact with the MLF; others, which were located a short distance away from the MLF, had axons projecting to the MLF tracts (Fig. 4J), showing that migrating motor neurons also extend axons. A time-lapse study using hindbrain explants (Bingham et al., 2005) (see Materials and methods) confirmed that the motor neurons were always located near the pial surface of the hindbrain during migration (Fig. 5A, see also Movie S1 in the supplementary material).

By contrast, in the *olt* and *ord* embryos, the nVII motor neurons did not migrate caudally near the pial surface of the hindbrain. Instead, they mismigrated towards the ventricle of the hindbrain at r4 (Fig. 4B,C,E,F). Some of the mismigrating neurons almost reached the midline at r4 or r5 (arrowheads in Fig. 4H,K; compare with the wild-type embryo in Fig. 4J). However, the nVII motor neurons located away from the pial surface of the hindbrain still projected axons to the MLF (arrows in Fig. 4H). The peripheral axons extended dorsally and laterally from the cell bodies of the nVII motor neurons, and they exited the hindbrain at r4 in the *olt* embryos (see Fig. S4 in the supplementary material). These results suggest that the *fz3a* and *celsr2* genes regulate the pathway of migrating nVII motor neurons without affecting their axogenesis.

nVII motor neurons migrate in aberrant directions by extending radial processes in the mutant embryos

In the wild-type embryos, the migrating nVII motor neurons showed biased caudal protrusive activity (see Movie S1 in the supplementary material) (Jessen et al., 2002). Our time-lapse observations revealed that the nVII motor neurons migrated dorsally in the hindbrain explants from the *olt* embryos (arrow in Fig. 5B, see Movie S2 in the supplementary material). Moreover, the motor neurons migrated aberrantly by extending long processes towards the ventricle at r4 (Fig. 5C, Movie S5 in the supplementary material). On average, 1.7 processes per embryo were observed at a single time point (Fig. 4M,O; 27 *olt* embryos were observed). A large proportion (47%; *n*=47) of these aberrant radial processes reached the ventricular surface (Fig. 4M). By contrast, radial processes were seldom observed in the wild-type embryos (Fig. 4L,O, see Movie S4 in the supplementary material). Only two aberrant processes were detected in 39 wild-type embryos and they did not reach the ventricular surface. The *ord* embryos injected with *celsr1a*-MO and *celsr1b*-MO showed an identical phenotype to that of the *olt* embryos (Fig. 4O; on average, 1.7 processes per embryo were observed in 24 morphants). These results suggest that the *fz3a* and *celsr* genes function in the same manner.

Next, we quantified the direction of the aberrant processes in the *olt* embryos. Most of the nVII motor neurons extended aberrant processes at right angles to the ventricular surface (Fig. 4N,P). Mismigrating motor neurons sometimes reached the ventricles (arrowhead in Fig. 4H), indicating that these aberrant processes could steer the migrating motor neurons in the wrong direction.

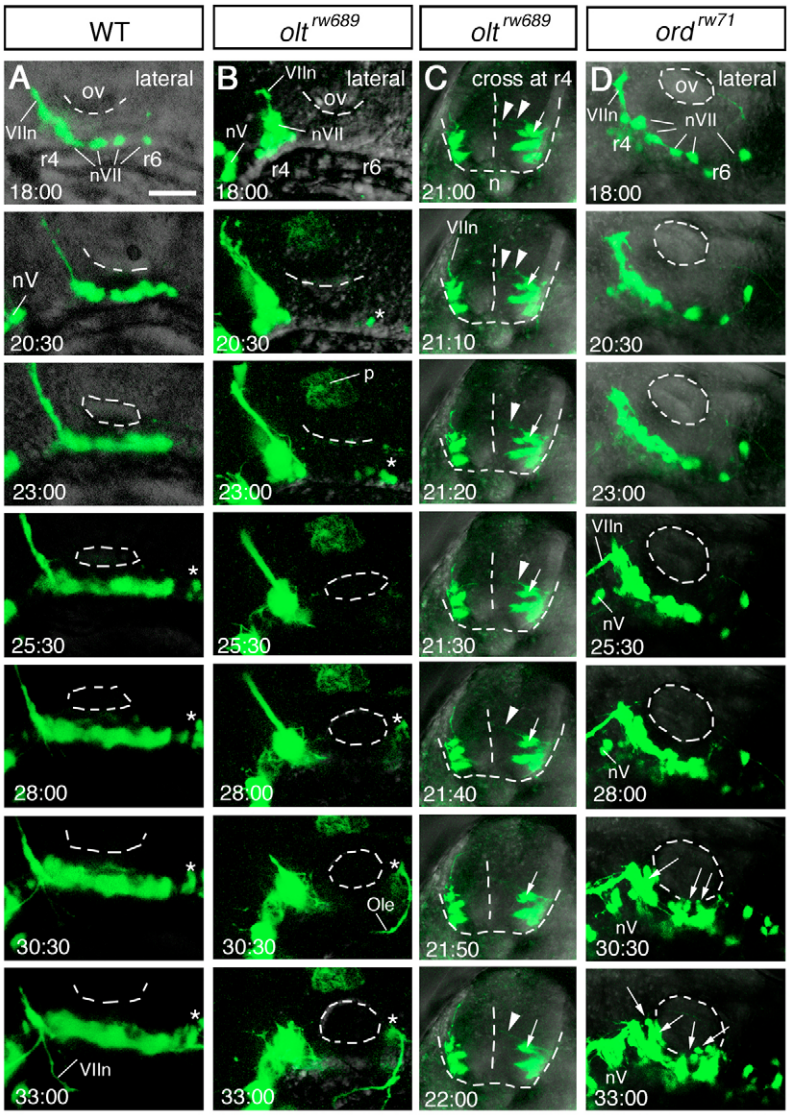

Fig. 5. Time-lapse analyses of defective migration of the nVII motor neurons. (**A-D**) Time-lapse observations of migrating nVII motor neurons in hindbrain explants of the wild-type (A), *olt* (B,C) and *ord* (D) Isl1-GFP embryos at the time (hpf) indicated in each panel. (Also see Movies S1-S5 in the supplementary material.) Images are composite stacks of serial optical sections. (A,B,D) Lateral views with anterior to the left; the inner lumen of the otic vesicle (ov) is indicated by broken lines. (C) Frontal views at r4. In the *olt* embryos, all neurons failed to migrate caudally (B) but mismigrated towards the ventricle (arrows in C) by extending aberrant radial processes (arrowheads in C). In the *ord* embryo, some of the late-born nVII motor neurons (indicated by arrows in D) migrated caudally in the dorsal part of the hindbrain. nV, trigeminal motor neurons; VIIn, facial motor axons. Asterisks indicate the r6-derived putative octavolateralis efferent (Ole) neurons (Wada et al., 2005). Scale bar: 50 μm.

Incomplete migration of nVII motor neurons in *ord* embryos

Next, we performed time-lapse observations of hindbrain explants from *ord* embryos. As described above, some of the nVII motor neurons migrated into r5 in the *ord* embryos because of the functional redundancy of *celsr1a* and *celsr1b* (Fig. 3H-L). These incompletely migrated neurons were not associated with the pial surface of the hindbrain (Fig. 4K).

The time-lapse observations revealed that some of the early-born nVII motor neurons migrated near the pial surface of the hindbrain in the *ord* embryos (Fig. 5D; also see Movie S3 in the supplementary material). By contrast, most of the late-born nVII motor neurons became detached from the pial surface of the hindbrain, and these motor neurons still migrated caudally to some extent (arrows in Fig. 5D; also see Movie S3 in the supplementary material). However, the migration of these nVII motor neurons in the *ord* embryos was by no means normal in nature, and most of the motor neurons stopped migrating at r5 and failed to reach r6.

We previously traced cell movements in wild-type embryos and showed that nVII motor neurons migrate independently of other neuroepithelial structures (Wada et al., 2005). To compare the behavior of nVII motor neurons with neighboring neuroepithelial cells, we observed mosaic embryos in which several neuroepithelial cells were randomly labeled with rhodamine-conjugated dextran (see Fig. S3A,B in the supplementary material). We confirmed that, in the *ord* embryos, some of the nVII motor neurons became detached from the pial surface of the brain and migrated caudally relative to the neighboring cells (see Fig. S3B in the supplementary material). These results demonstrated that the nVII motor neurons can migrate caudally to some extent without keeping direct contact with the pial structure of the hindbrain in the *ord* embryos. However, we can not exclude the possibility that some component of the pial structures, such as the MLF, may have a long-distance influence.

fz3a and *celsr2* genes mainly act in a non-cell-autonomous manner during migration of nVII motor neurons

During the development of zebrafish embryos, the hindbrain everts, and its ventricle opens at 18-22 hpf and begins to expand at 24 hpf (Lowery and Sive, 2005). The *olt* embryos also showed rapid expansion of the ventricle (as observed in the wild-type embryos) when they were stained with anti-β-catenin antibody at 24 hpf and 33 hpf (Fig. 6A,B) (Lowery and Sive, 2005). As a consequence, the orientation of the neuroepithelial cells became more parallel to the

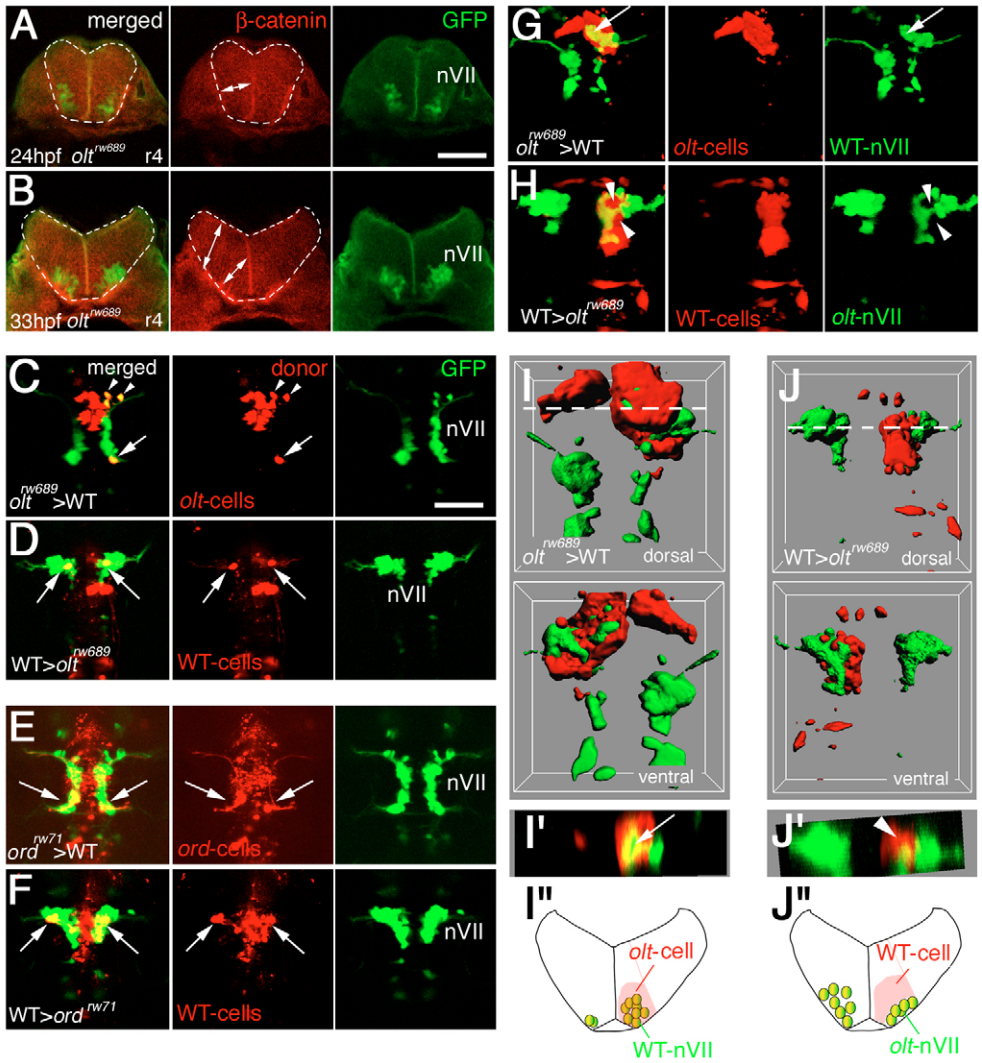

Fig. 6. Functional *fz3a* and *celsr2* genes in neuroepithelial cells are required for preventing integration of nVII motor neurons into the neuroepithelium. (**A**,**B**) Single focal-plane images of cross sections at r4 in *olt* Isl1-GFP embryos stained with anti-β-catenin antibody (red) at 24 (A) and 33 (B) hpf. Orientation of the neuroepithelial cells is shown by double-headed arrows. Hindbrain regions are outlined by broken lines. (**C-F**) Mosaic experiments were performed to determine the cell autonomy of the *olt* and *ord* genes. The donor cells were labeled with rhodamine-conjugated dextran (red). The nVII motor neurons (arrows) derived from the *olt*^{rw689} (C) and *ord*^{rw71} (E) Isl1-GFP embryos migrated caudally in the wild-type host embryos, although some were still located in r4 at the time of observation (arrowheads in C). By contrast, none of the wild-type-derived nVII motor neurons (arrows) reached r6 in the *olt* (D) and *ord* (F) host embryos. Red puncta signals may be the debris of the dead transplanted cells. However, as we observed the growth of the peripheral axons of the nVII motor neurons in each mosaic embryo (see Materials and methods), it is unlikely that such debris had serious adverse effects on the development of these embryos. Dorsal views of the embryos are shown. (**G-J**) Embryos showing mosaicism in the neuroepithelium at the r4 region. When the *olt*-derived cells were incorporated into the neuroepithelium of the wild-type host embryos at r4, the nVII motor neurons migrated aberrantly into the mutant neuroepithelium (arrows in G and I′). By contrast, when wild-type-derived cells were incorporated into the r4 region of the *olt* host embryos, the nVII motor neurons failed to invade the wild-type neuroepithelium (arrowheads in H and J′). (C-H) Images are composite stacks of serial optical sections. (I,J) Computationally reconstructed 3D images of the embryos shown in G and H. Dorsal and ventral views of the embryos are shown. In I, mismigrated nVII motor neurons (green) are hidden by the surrounding *olt* embryo-derived neuroepithelial cells (red) as no transparency was given to the images of the donor-cell clusters. (**I′**,**J′**) Computationally reconstructed cross sections at r4 indicated by the broken line in I and J. (**I″**,**J″**) Schematic cross sections at r4 of the embryos shown in G and H, respectively. The yellow signals in the merged panels of G and H are technical artifacts caused by the superimposition of the red signals of the donor cells and the green signals of the motor neurons. As red signals were not detected in the axons of the motor neurons (G,H, middle panels), all of the nVII motor neurons were derived from the host embryos. Scale bars: 50 μm in A for A,B; and 50 μm in C for C-H.

midline, and the nVII motor-neuron clusters changed their positions to be relatively further away from the ventricle and the neurons were located laterally in the *olt* embryos (Fig. 6B).

We investigated the cell autonomy of the mutations by mosaic analysis (see Fig. S3C,C′ in the supplementary material for imaging of the shapes of the transplanted neuroepithelial cells). As described above, none (or almost none) of the nVII motor neurons had reached the r6 region in the *olt* and *ord* mutant embryos at 48 hpf (Fig. 1D-F). However, a significant proportion of the MZ-*olt*-derived neurons (45% of 29 neurons monitored in four mosaic embryos), or of the MZ-*ord*-derived neurons (56% of 75 neurons monitored in nine mosaic embryos), had migrated into r6 in the wild-type host embryos at 36 hpf (Fig. 6C,E, also see Fig. S5A,C in the supplementary material for observations of other mosaic embryos). Because some of the late-born neurons remained in r4 or r5 at the time of observation (arrowheads in Fig. 6C), we could not completely exclude the cell-autonomous involvement of these genes in the migration of the nVII motor neurons. By contrast, none (or almost none) of the wild-type-derived nVII motor neurons reached r6 in the MZ-*olt* host embryos (0% of 31 neurons monitored in eight mosaic embryos) or the MZ-*ord* host embryos (1.5% of 65 neurons monitored in six mosaic embryos) (Fig. 6D,F, also see Fig. S5B,D in the supplementary material for observations of other mosaic embryos). These results indicate that the *fz3a* and *celsr2* genes mainly act in a non-cell-autonomous manner during migration of nVII motor neurons.

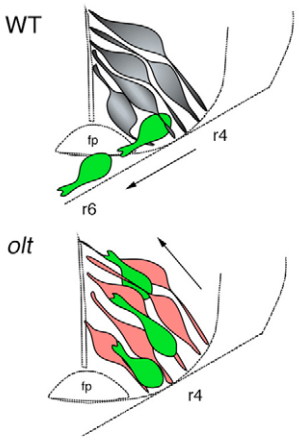

Fig. 7. Schematic drawing of nVII motor-neuron migration in the wild-type and *olt* embryos. In the wild-type embryos, the nVII motor neurons (green) migrated caudally near the pial surface of the hindbrain. By contrast, in the *olt* embryos, because the neuroepithelial cells (red) had lost their ability to prevent integration of the nVII motor neurons, the motor neurons migrated towards the ventricle by extending aberrant processes radially to the ventricle. Directions of migration of the nVII motor neurons are indicated by arrows. See text for details.

fz3a is required in the neuroepithelial cells to restrict the nVII motor neurons near the pial surface of the hindbrain

We then investigated the cell type responsible for regulating the migration of the nVII motor neurons in the developing hindbrain. Because *fz3a* and *celsr2* mRNAs are expressed widely in the hindbrain (Fig. 2E,E′; Fig. 3E,E′), the neuroepithelial cells surrounding the nVII motor neurons are good candidates as regulators of nVII motor-neuron migration. In the mutant embryos, the nVII motor neurons migrated into the neuroepithelial layer at r4 (Fig. 4E,F). A function of wild-type neuroepithelium may, therefore, be to prevent integration of the nVII motor neurons into the neuroepithelium and restrict them near the pial surface of the brain.

To test this hypothesis, we observed the behavior of nVII motor neurons in wild-type embryos in which the neuroepithelium contained MZ-*olt*-derived cells in mosaic analyses (Fig. 6G,I-I″). In these experiments, we analyzed MZ-*olt* embryos because the *ord* embryos showed complex migrating behavior, as shown in Fig. 5D. The MZ-*olt*-derived cells (red) were incorporated into the neuroepithelium of the wild-type host embryos at r4 (Fig. 6G). In the intact side (left side of the embryo shown in Fig. 6G), the wild-type nVII motor neurons (green) were located normally – near the pial surface of the brain, as described (Fig. 4A,D). However, in the mosaic region (right side of the embryo shown in Fig. 6G), the wild-type nVII motor neurons mismigrated into the MZ-*olt*-derived cell cluster (Fig. 6G,I,I′; the example shown is representative of six mosaic embryos). Because of the eversion of the hindbrain as described above (Fig. 6A,B), these mismigrated nVII motor neurons were located dorsally rather than medially in the hindbrain (Fig. 6G). These results showed that the mutant neuroepithelial cells allowed invasion of the wild-type nVII motor neurons into the neuroepithelial layer (Fig. 6I″).

Next, we observed the behavior of nVII motor neurons in *olt* embryos in which the neuroepithelium contained wild-type-derived cells (Fig. 6H,J-J″). In this case, the wild-type-derived cells (red) were incorporated into the neuroepithelium of the MZ-*olt* host embryos at r4 and r5 (Fig. 6H). In the intact side (left side of the embryo shown in Fig. 6H), the nVII motor neurons (green) mismigrated dorsally in the *olt* mutant neuroepithelium, as described (Fig. 4B,E). However, in the mosaic region (right side of the embryo shown in Fig. 6H), the MZ-*olt*-derived nVII motor neurons failed to invade the wild-type cell cluster (Fig. 6H,J,J′; the example shown is representative of ten mosaic embryos; also see Fig. S6 in the supplementary material for observations of other mosaic embryos). These results showed that the wild-type neuroepithelial cells prevented the nVII motor neurons from invading the neuroepithelial layer (Fig. 6J″). In Fig. 6H, it is apparent that several nVII motor neurons in the mosaic regions migrated slightly caudally in comparison with the intact side, suggesting that the caudal migration may be rescued by the associated wild-type neuroepithelium. However, we could not introduce wild-type large-cell clusters encompassing the r4 and r5 regions in the other mosaic embryos. Therefore, we could not make sufficient observations to provide statistical support for this possibility.

Together, the above results demonstrate that the *fz3a* gene acts in the neuroepithelium to regulate the direction of neuronal migration by preventing integration of nVII motor neurons into the neuroepithelium and by restricting them to a region near the pial surface of the brain (Fig. 7).

DISCUSSION

Neuroepithelial cells prevent integration of nVII motor neurons into the neuroepithelium

Previous studies from our, and other, laboratories revealed that the normal migration of the nVII motor neurons is guided by two mechanisms. In mouse hindbrain, guidance cues emanate from r5 and r6 to attract the nVII motor neurons (Studer, 2001). These may include Reelin (Ohshima et al., 2002; Rossel et al., 2005) and Sdf-1 (Sapede et al., 2005) signaling. In the present study, we have clearly shown that the neuroepithelial cells function in preventing integration of the nVII motor neurons into the neuroepithelial layer of the hindbrain, and that this radial exclusion is essential for normal migration of the nVII motor neurons. The mosaic experiments using *tri/stbm* (Jessen et al., 2002), *llk/scrb1* (Wada et al., 2005), *olt/fz3a* and *ord/celsr2* (present study) genes showed that the wild-type-derived nVII motor neurons completely failed to migrate caudally in the mutant host embryos. We showed that the nVII motor neurons of MZ-*olt* host embryos did not invade the wild-type neuroepithelial cell cluster but that, conversely, the nVII motor neurons of wild-type host embryos did invade the mutant neuroepithelial cell cluster (Fig. 6G-J). These findings indicate that normal migration requires a functional *olt/fz3a* gene mainly in the surrounding neuroepithelial cells. However, as a non-negligible proportion of the mutant embryo-derived nVII motor neurons also failed to migrate in the wild-type host embryos (Fig. 6C), we can not exclude the possibility that these genes may also act in the migrating nVII motor neurons themselves.

We observed that some of the early-born nVII motor neurons mismigrated radially away from the pial surface in the *olt* embryos (Fig. 5C). However, we can still not exclude the possibility that some other late-born neurons may have stalled during migration on their way to the pial surface, before they started expressing GFP.

Neuroepithelial cells play a contrasting role for the re-integration of newly divided neuroepithelial cells

It has been shown that the *tri/stbm* gene in neuroepithelial cells regulates the re-integration of daughter cells into the neuroepithelial layer after cell division (Ciruna et al., 2006). By contrast,

neuroepithelial cells prevent integration of nVII motor neurons into the neuroepithelial layer, as shown in the present study. Hence, we propose opposite roles for the neuroepithelial cells depending on the cell type that they act upon – integration of neuroepithelial daughter cells into the neuroepithelial layer and exclusion of nVII motor neurons from the neuroepithelial layer. Fz3a and Celsr2 together with Stbm may control cell-adhesion or cell-repulsion molecules that are specifically required for the integration or exclusion of cells from the neuroepithelium.

Radial exclusion and caudal migration of the nVII motor neurons are interdependent mechanisms

We showed that in the *olt* embryos, the mismigrated nVII motor neurons extended aberrant processes towards the ventricle at right angles to the anterior-posterior axis (Fig. 4N,P). These observations suggest that the nVII motor neurons in the *olt* embryos lose their ability to migrate caudally. There was some, albeit incomplete, migration of the nVII motor neurons in the *ord* embryos, apparently because of functional redundancy with the *celsr1a* and *celsr1b* genes. However, the migration of the nVII motor neurons in the *ord* embryos was by no means normal in nature, and these neurons stopped migrating at r5 and failed to reach r6. In the *ord* embryos, the nVII motor neurons also invaded the neuroepithelial layer. These results suggest that radial exclusion and caudal migration are interdependent mechanisms of normal nVII motor neuron migration. A recent study has shown that the *tri/stbm* gene is essential for localization of Prickle to the anterior membrane of neuroepithelial cells (Ciruna et al., 2006), suggesting that these genes may control the anterior-posterior polarity of these cells (Ciruna et al., 2006). This might provide some basis for caudal migration of the nVII motor neurons.

In a previous study, we showed that the r4-derived nVII motor neurons are composed of the branchiomotor neurons and the OLe neurons (Higashijima et al., 2000; Wada et al., 2005), and that the OLe neurons are possibly among the population to first migrate out of r4 (Fig. 5D). However, by labeling the OLe neurons with DiI retrogradely, we demonstrated that the OLe neurons failed to migrate caudally and remained in r4 in the *ord* embryos (n=4, see Fig. S7 in the supplementary material).

Possible roles of the *fz3a* and *celsr* genes in the neuroepithelium

We showed that maternal and zygotic impairment of Fz3a, or overexpression of Fz3a-ΔC, specifically disrupted nVII motor-neuron migration without affecting the early pattern formations or CE movements during gastrulation (Fig. 1B; Fig. 2I). These results suggest that Fz3a interacts with only a specific ligand to regulate the neuroepithelial functions. Conversely, Silberblick (Slb)/Wnt11 and Pipetail (Ppt)/Wnt5a regulate CE movements but do not regulate nVII motor-neuron migration (Bingham et al., 2002; Jessen et al., 2002). Our data, taken together with these results, suggest that the genetic cascades regulating the neuroepithelial functions adopt a different ligand-receptor system to that used for the regulation of CE movements.

It remains unclear as to how the other downstream effectors of Fz3a, including Dsh, are involved in the regulation of neuroepithelial functions. We showed that simultaneous overexpression of Fz3a and *Xenopus* Dsh (Xdsh) led to the recruitment of Xdsh to the plasma membrane at the blastula stages (see Fig. S2B in the supplementary material). These results suggest that Fz3a can interact with Xdsh. By contrast, overexpression of a mutant form of Xdsh, Xdd1, which lacks a PDZ domain disrupts CE movements in a dominant-negative manner but does not impair migration of the nVII motor neurons (Jessen et al., 2002). Therefore, there may be functional specialization among different Dsh proteins in zebrafish, as described above for Wnts and Fzs, and *Xenopus*-derived Xdd1 may antagonize a special Dsh that is required for CE movements only. Alternatively, the domains of Dsh required for the neuroepithelial functions may be different from those regulating CE movements, and Xdd1 may still be able to transmit signals that normally regulate neuroepithelial functions. We also do not exclude the possibility that Fz3a may act independently of Dsh in its regulation of neuroepithelial functions.

It has been suggested that homophilic interaction of Fmi through the extracellular cadherin-repeat domain plays an important role at cell-cell boundaries in epithelial planar polarity (Usui et al., 1999). Thus, it is possible that the Celsr proteins also regulate cell adhesion between adjacent neuroepithelial cells to restrict invasion of the nVII motor neurons into the neuroepithelium.

The Eph receptors and their ligands, the ephrins, are other good candidate mediators of cell repulsion (for reviews, see Wilkinson, 2001; Kullander and Klein, 2002). In the mouse and chick hindbrain, Eph receptors and ephrin ligands are expressed in the nVII motor neurons and neuroepithelial cells, respectively (Cowan et al., 2000; Kury et al., 2000). Recent studies have shown that Dsh forms a complex with EphrinB to mediate cell repulsion in *Xenopus* embryos (Tanaka et al., 2003; Lee et al., 2006). Thus, it is possible that Fz and Celsrs may regulate the activity of cell-repulsive molecules, such as ephrins, on the surface of the neuroepithelial cells.

Novel roles of the frizzled and celsr family genes in brain development

Our present finding that neuroepithelial cells are involved in positioning specific neurons near the pial surface suggests a fundamental role for the neuroepithelium in brain development. In the mammalian cortex, neurons are generated in ventricular germinal zones and migrate radially towards the pial surface to form architectural layered structures. In mouse embryos, Reelin signaling regulates the positioning of neurons during layer formation of the cerebrum (reviewed by Tissir and Goffinet, 2003), and is essential for radial migration of the nVII motor neurons (Ohshima et al., 2002; Rossel et al., 2005). These data suggest that similar mechanisms regulate the proper positioning of both the hindbrain motor neurons and the cortical layer neurons.

In the mouse cerebral cortex, many wnt and frizzled family genes are expressed in gene-specific regional and lamina patterns (Shimogori et al., 2004). Such patterned expression suggests the possibility that these genes are involved in other aspects of brain development. Recent studies have shown that functional *fzd3* and *celsr3* genes are required for the development of the anterior commissure, and the cortico-subcortical, thalamocortical and corticospinal tracts (Wang et al., 2002; Tissir et al., 2005). It is possible that the mouse *fzd3* and *celsr3* genes regulate neuroepithelial cells to guide these axonal tracts to the proper region in a similar manner to that by which the zebrafish *fz3a* and *celsr* genes act in neuroepithelial cells to restrict the migrating nVII motor neurons near the pial surface of the hindbrain. Our demonstration of a role for neuroepithelial cells in preventing integration of differentiated neurons into the neuroepithelial layer may provide new insights into the general mechanisms underlying the formation of layered structures in the mammalian brain, such as in the cerebral cortex.

We thank J. Kuwada, T. Jowett, C. Moens, M. Tada and A. Miyawaki for gifts of cDNA clones; A. Shimada for technical assistance; and M. Tada and A. Thomson for discussion and critical reading of the manuscript. This research was supported in part by Grant-in-Aid and a Special Coordination Fund from

the Ministry of Education, Science, Technology, Sports and Culture of Japan; and by grants for Core Research for Evolutional Science and Technology from Japan Science and Technology Corporation (JST).

Supplementary material

Supplementary material for this article is available at http://dev.biologists.org/cgi/content/full/133/23/4749/DC1

References

Axelrod, J. D., Miller, J. R., Shulman, J. M., Moon, R. T. and Perrimon, N. (1998). Differential recruitment of Dishevelled provides signaling specificity in the planar cell polarity and Wingless signaling pathways. *Genes Dev.* **12**, 2610-2622.

Bingham, S., Higashijima, S., Okamoto, H. and Chandrasekhar, A. (2002). The Zebrafish *trilobite* gene is essential for tangential migration of branchiomotor neurons. *Dev. Biol.* **242**, 149-160.

Bingham, S. M., Toussaint, G. and Chandrasekhar, A. (2005). Neuronal development and migration in zebrafish hindbrain explants. *J. Neurosci. Methods* **149**, 42-49.

Carreira-Barbosa, F., Concha, M. L., Takeuchi, M., Ueno, N., Wilson, S. W. and Tada, M. (2003). Prickle 1 regulates cell movements during gastrulation and neuronal migration in zebrafish. *Development* **130**, 4037-4046.

Chandrasekhar, A., Moens, C. B., Warren, J. T., Jr, Kimmel, C. B. and Kuwada, J. Y. (1997). Development of branchiomotor neurons in zebrafish. *Development* **124**, 2633-2644.

Chen, C. M., Strapps, W., Tomlinson, A. and Struhl, G. (2004). Evidence that the cysteine-rich domain of *Drosophila* Frizzled family receptors is dispensable for transducing Wingless. *Proc. Natl. Acad. Sci. USA* **101**, 15961-15966.

Ciruna, B., Jenny, A., Lee, D., Mlodzik, M. and Schier, A. F. (2006). Planar cell polarity signalling couples cell division and morphogenesis during neurulation. *Nature* **439**, 220-224.

Cowan, C. A., Yokoyama, N., Bianchi, L. M., Henkemeyer, M. and Fritzsch, B. (2000). EphB2 guides axons at the midline and is necessary for normal vestibular function. *Neuron* **26**, 417-430.

Dann, C. E., Hsieh, J. C., Rattner, A., Sharma, D., Nathans, J. and Leahy, D. J. (2001). Insights into Wnt binding and signalling from the structures of two Frizzled cysteine-rich domains. *Nature* **412**, 86-90.

Formstone, C. J. and Little, P. F. (2001). The flamingo-related mouse Celsr family (Celsr1-3) genes exhibit distinct patterns of expression during embryonic development. *Mech. Dev.* **109**, 91-94.

Formstone, C. J. and Mason, I. (2005). Combinatorial activity of Flamingo proteins directs convergence and extension within the early zebrafish embryo via the planar cell polarity pathway. *Dev. Biol.* **282**, 320-335.

Goutel, C., Kishimoto, Y., Schulte-Merker, S. and Rosa, F. (2000). The ventralizing activity of Radar, a maternally expressed bone morphogenetic protein, reveals complex bone morphogenetic protein interactions controlling dorso-ventral patterning in zebrafish. *Mech. Dev.* **99**, 15-27.

Hatten, M. E. (2002). New directions in neuronal migration. *Science* **297**, 1660-1663.

Higashijima, S., Hotta, Y. and Okamoto, H. (2000). Visualization of cranial motor neurons in live transgenic zebrafish expressing green fluorescent protein under the control of the islet-1 promoter/enhancer. *J. Neurosci.* **20**, 206-218.

Jessen, J. R., Topczewski, J., Bingham, S., Sepich, D. S., Marlow, F., Chandrasekhar, A. and Solnica-Krezel, L. (2002). Zebrafish *trilobite* identifies new roles for Strabismus in gastrulation and neuronal movements. *Nat. Cell Biol.* **4**, 610-615.

Klein, T. J. and Mlodzik, M. (2005). PLANAR CELL POLARIZATION: an emerging model points in the right direction. *Annu. Rev. Cell Dev. Biol.* **21**, 155-176.

Kriegstein, A. R. and Noctor, S. C. (2004). Patterns of neuronal migration in the embryonic cortex. *Trends Neurosci.* **27**, 392-399.

Kullander, K. and Klein, R. (2002). Mechanisms and functions of Eph and ephrin signalling. *Nat. Rev. Mol. Cell Biol.* **3**, 475-486.

Kury, P., Gale, N., Connor, R., Pasquale, E. and Guthrie, S. (2000). Eph receptors and ephrin expression in cranial motor neurons and the branchial arches of the chick embryo. *Mol. Cell. Neurosci.* **15**, 123-140.

Langenberg, T., Brand, M. and Cooper, M. S. (2003). Imaging brain development and organogenesis in zebrafish using immobilized embryonic explants. *Dev. Dyn.* **228**, 464-474.

Lee, H. S., Bong, Y. S., Moore, K. B., Soria, K., Moody, S. A. and Daar, I. O. (2006). Dishevelled mediates ephrinB1 signalling in the eye field through the planar cell polarity pathway. *Nat. Cell Biol.* **8**, 55-63.

Lowery, L. A. and Sive, H. (2005). Initial formation of zebrafish brain ventricles occurs independently of circulation and requires the nagie oko and snakehead/atp1a1a.1 gene products. *Development* **132**, 2057-2067.

Moens, C. B., Yan, Y. L., Appel, B., Force, A. G. and Kimmel, C. B. (1996). valentino: a zebrafish gene required for normal hindbrain segmentation. *Development* **122**, 3981-3990.

Moens, C. B., Cordes, S. P., Giorgianni, M. W., Barsh, G. S. and Kimmel, C. B. (1998). Equivalence in the genetic control of hindbrain segmentation in fish and mouse. *Development* **125**, 381-391.

Nagai, T., Ibata, K., Park, E. S., Kubota, M., Mikoshiba, K. and Miyawaki, A. (2002). A variant of yellow fluorescent protein with fast and efficient maturation for cell-biological applications. *Nat. Biotechnol.* **20**, 87-90.

Nasevicius, A. and Ekker, S. C. (2000). Effective targeted gene 'knockdown' in zebrafish. *Nat. Genet.* **26**, 216-220.

Ohshima, T., Ogawa, M., Takeuchi, K., Takahashi, S., Kulkarni, A. B. and Mikoshiba, K. (2002). Cyclin-dependent kinase 5/p35 contributes synergistically with Reelin/Dab1 to the positioning of facial branchiomotor and inferior olive neurons in the developing mouse hindbrain. *J. Neurosci.* **22**, 4036-4044.

Oxtoby, E. and Jowett, T. (1993). Cloning of the zebrafish krox-20 gene (krx-20) and its expression during hindbrain development. *Nucleic Acids Res.* **21**, 1087-1095.

Park, T. J., Gray, R. S., Sato, A., Habas, R. and Wallingford, J. B. (2005). Subcellular localization and signaling properties of dishevelled in developing vertebrate embryos. *Curr. Biol.* **15**, 1039-1044.

Prince, V. E., Moens, C. B., Kimmel, C. B. and Ho, R. K. (1998). Zebrafish hox genes: expression in the hindbrain region of wild-type and mutants of the segmentation gene, valentino. *Development* **125**, 393-406.

Rossel, M., Loulier, K., Feuillet, C., Alonso, S. and Carroll, P. (2005). Reelin signaling is necessary for a specific step in the migration of hindbrain efferent neurons. *Development* **132**, 1175-1185.

Rothbacher, U., Laurent, M. N., Deardorff, M. A., Klein, P. S., Cho, K. W. and Fraser, S. E. (2000). Dishevelled phosphorylation, subcellular localization and multimerization regulate its role in early embryogenesis. *EMBO J.* **19**, 1010-1022.

Sapede, D., Rossel, M., Dambly-Chaudiere, C. and Ghysen, A. (2005). Role of SDF1 chemokine in the development of lateral line efferent and facial motor neurons. *Proc. Natl. Acad. Sci. USA* **102**, 1714-1718.

Shima, Y., Copeland, N. G., Gilbert, D. J., Jenkins, N. A., Chisaka, O., Takeichi, M. and Uemura, T. (2002). Differential expression of the seven-pass transmembrane cadherin genes Celsr1-3 and distribution of the Celsr2 protein during mouse development. *Dev. Dyn.* **223**, 321-332.

Shimoda, N., Knapik, E. W., Ziniti, J., Sim, C., Yamada, E., Kaplan, S., Jackson, D., de Sauvage, F., Jacob, H. and Fishman, M. C. (1999). Zebrafish genetic map with 2000 microsatellite markers. *Genomics* **58**, 219-232.

Shimogori, T., VanSant, J., Paik, E. and Grove, E. A. (2004). Members of the Wnt, Fz, and Frp gene families expressed in postnatal mouse cerebral cortex. *J. Comp. Neurol.* **473**, 496-510.

Studer, M. (2001). Initiation of facial motoneurone migration is dependent on rhombomeres 5 and 6. *Development* **128**, 3707-3716.

Tanaka, M., Kamo, T., Ota, S. and Sugimura, H. (2003). Association of Dishevelled with Eph tyrosine kinase receptor and ephrin mediates cell repulsion. *EMBO J.* **22**, 847-858.

Tissir, F. and Goffinet, A. M. (2003). Reelin and brain development. *Nat. Rev. Neurosci.* **4**, 496-505.

Tissir, F., Bar, I., Jossin, Y., De Backer, O. and Goffinet, A. M. (2005). Protocadherin Celsr3 is crucial in axonal tract development. *Nat. Neurosci.* **8**, 451-457.

Tree, D. R., Ma, D. and Axelrod, J. D. (2002). A three-tiered mechanism for regulation of planar cell polarity. *Semin. Cell Dev. Biol.* **13**, 217-224.

Trevarrow, B., Marks, D. L. and Kimmel, C. B. (1990). Organization of hindbrain segments in the zebrafish embryo. *Neuron* **4**, 669-679.

Usui, T., Shima, Y., Shimada, Y., Hirano, S., Burgess, R. W., Schwarz, T. L., Takeichi, M. and Uemura, T. (1999). Flamingo, a seven-pass transmembrane cadherin, regulates planar cell polarity under the control of Frizzled. *Cell* **98**, 585-595.

Wada, H., Iwasaki, M., Sato, T., Masai, I., Nishiwaki, Y., Tanaka, H., Sato, A., Nojima, Y. and Okamoto, H. (2005). Dual roles of zygotic and maternal Scribble1 in neural migration and convergent extension movements in zebrafish embryos. *Development* **132**, 2273-2285.

Wang, Y., Thekdi, N., Smallwood, P. M., Macke, J. P. and Nathans, J. (2002). Frizzled-3 is required for the development of major fiber tracts in the rostral CNS. *J. Neurosci.* **22**, 8563-8573.

Warren, J. T., Jr, Chandrasekhar, A., Kanki, J. P., Rangarajan, R., Furley, A. J. and Kuwada, J. Y. (1999). Molecular cloning and developmental expression of a zebrafish axonal glycoprotein similar to TAG-1. *Mech. Dev.* **80**, 197-201.

Westerfield, M. (2000). *The Zebrafish Book* (4th edn). Eugene, OR: University of Oregon.

Wilkinson, D. G. (2001). Multiple roles of EPH receptors and ephrins in neural development. *Nat. Rev. Neurosci.* **2**, 155-164.